PHYS4610 Senior Project I
Simulation of Astrophysical Fluid

Man Tsun, Wu
Department of Physics, The Chinese University of Hong Kong, Shatin, New Territories, Hong Kong
(Dated: December 2019)

I. INTRODUCTION

Fluid dynamics is important and universal in nature, especially when dealing with many astrophysical problems, in order to study the collective behaviour of fluids on large scales[1]. Astrophysical fluid dynamics is a branch of astronomy to study astrophysical fluids, which are the fluids found in outer space, such as the motion of a collection of stars or nebulae in interstellar space.

Three hydrodynamic systems were verified with the theory of fluid dynamics qualitatively and quantitatively by computer simulations, namely the sound wave propagation, the Sod shock tube problem and the Kelvin-Helmholtz instability. Inviscid, irrotational, incompressible and ideal fluids were assumed. The PLUTO code, which is an applicable software to solve fluid dynamics equations was utilized to perform the simulations. Gnuplot was used to visualize the simulation results for discussion and verifying the theoretical results.

The paper is structured as follows: Section II introduces the definition of fluid and the basic fluid dynamics equations; Section III introduces the PLUTO code and the code design; Section IV introduces the sound wave simulation, including the sound wave equations and initialization, the simulation results and discussion; Section V introduces the Sod shock tube problem, including the expected phenomenons of shock wave, contact discontinuity and rarefraction wave, the simulation results and the convergence rate compared to the theoretical values; Section VI introduces the Kelvin-Helmholtz instability, including a brief derivation of the dispersion relation and the comparison of different results using different initialization parameters; and Section VII concludes the above simulations and the states the outlook of further studies.

II. BASIC FLUID DYNAMICS

A. Definition of Fluid

Fluids are substance that can flow, such as liquids and gases. Unlike solid, they do not have rigidity. Fluids cannot sustain tangential force and will flow if shear force is applied. In order to describe the fluid dynamics of a collection of particles, a continuum description is essential. An effectively continuous medium could be treated if the size of the domain of interest is much larger than the mean free path λ, which is the average distance travelled by the particles between collisions. A fluid volume element could be defined and the continuous medium could be associated with the macroscopic properties such as the bulk velocity $\boldsymbol{u}$ and the density of the fluid element ρ, if the number of particles is large enough.

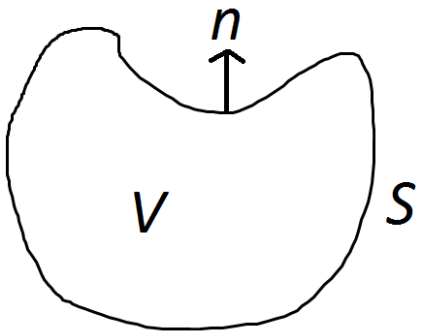

FIG. 1: A volume V enclosed by the surface S, with outward normal $\boldsymbol{n}$.

B. Basic equations

The macroscopic properties could be given as functions of position with respect to some fixed reference frame of time t. The Eulerian description focuses on the quantity at a particular point of space and at a particular time. Several basic Euler equations could be derived as follows.

1. *The continuity equation*

Figure 1 shows an arbitrary fluid element. By conservation of mass, the outward flux of mass of the fluid is equal to the rate of decrease of mass, where

$$\int_S \rho \boldsymbol{v} \cdot \boldsymbol{n} da = -\frac{d}{dt} \int V \rho d\tau. \tag{1}$$

By using divergence theorem, one could obtain the relation:

$$\frac{\partial \rho}{\partial t} + \nabla \cdot (\rho \boldsymbol{v}) = 0, \tag{2}$$

which is known as the continuity equation (conservation of mass equation).

2. The momentum equation

By Newton's second law or the conservation of momentum, the momentum equation is given by

$$\rho \frac{D\boldsymbol{v}}{Dt} = \boldsymbol{f}, \tag{3}$$

where $\boldsymbol{f}$ is the total force per unit volume acting on the fluid element. $\frac{D}{Dt}$ is the material derivative, which describes the rate of change following the trajectory of the fluid element. Thus $\frac{D\boldsymbol{v}}{Dt}$ is the acceleration of the fluid element when the fluid element move from $\boldsymbol{r}$ at time t to $\boldsymbol{r} + \boldsymbol{v}\delta t$. It could be shown that

$$\frac{D}{Dt} = \frac{\partial}{\partial t} + \boldsymbol{v} \cdot \nabla. \tag{4}$$

The body forces and the surface forces contribute to the net force acting on the fluid. The former relates to the external forces $\boldsymbol{f}_{ext}$ and the latter are the forces exerted on the surface S of the fluid element by the surrounding fluid due to the pressure gradient $-\nabla P$. Therefore, Eq (3) could be written as:

$$\frac{\partial \boldsymbol{v}}{\partial t} + (\boldsymbol{v} \cdot \nabla)\boldsymbol{v} = -\frac{1}{\rho}\nabla P + \frac{1}{\rho}\boldsymbol{f}_{ext}, \tag{5}$$

which is known as the Euler's equation of fluid motion of an inviscid, ideal fluid.

3. Energy equation

By multiplying the Newton's second law by $\boldsymbol{v}$, the rate of work is equal to the rate of change of kinetic energy, this could lead to the equation:

$$\frac{D}{Dt}(\frac{1}{2}\boldsymbol{v}^2) = -\frac{1}{\rho}\boldsymbol{v} \cdot \nabla P + \boldsymbol{v} \cdot \boldsymbol{f}_{ext}, \tag{6}$$

which is known as the mechanical energy equation.

The total energy is equal to the sum of kinetic and internal thermal energy. The rate of change of sum is equal to the rate of work done on the fluid by surface and body forces plus the rate at which heat is added to the fluid by a rate ϵ per uni mass within the fluid element and the heat flux $\boldsymbol{F}$ across the surface S. By using Eq (2), Eq (7) and divergence theorem, it could be shown that:

$$\frac{DU}{Dt} = \frac{P}{\rho^2}\frac{D\rho}{Dt} + \epsilon - \frac{1}{\rho}\nabla \cdot \boldsymbol{F}. \tag{7}$$

C. Hydrostatic Equilibrium

When the fluid is at rest, it is said to be hydrostatic equilibrium for $\boldsymbol{v} = 0$. The body force caused by the acceleration due to gravity is balanced with the gradient pressure. For the external force $\boldsymbol{f}_{ext} = \rho g$, Eq (5) becomes

$$\nabla P = \rho \boldsymbol{g}. \tag{8}$$

Eq (7) also implies that the fluid is said to be in thermal equilibrium as $\epsilon = \frac{1}{\rho}\nabla \cdot \boldsymbol{F}$.

III. THE PLUTO CODE

PLUTO code is a computation fluid code introduced in the 21$^{\text{st}}$ century to perform direct numerical simulations. The software claims to provide a multiphysics, multialgorithm and user friendly environment to seek solutions of the system of conservation law[2]. Attributes such as the boundary conditions, the geometry, the body force and physics module etc. could be set manually to define a specific problem.

For most physics problems, the exact solutions could be complicated, numerical approach is an alternative to the theoretical derivation. By inputting certain parameters and initialization of primitive variables of a set of conservative quantity $\boldsymbol{U}$, including the velocity vector $\boldsymbol{v}$, the density ρ and the pressure P in all space within the computational domain defined, the system evolves using the three conservation laws mentioned in Section II.

Different Riemann solvers and time-marching algorithms could be selected for desired computational time and accuracy. The most general form for the first order finite difference approximation is

$$\frac{\boldsymbol{U}^{n+1} - \boldsymbol{U}^n}{\delta t} = \mathcal{L}^n, \tag{9}$$

for step n to $n+1$. $\mathcal{L}$ is an operator relates to the conservation laws mentioned in Section II for the corresponding primitive variables. the time step δt is controlled by the Courant-Friedrichs-Lewy (CFL) condition, where the time step should be less than the time to travel across a grid spacing δx. For instant,

$$\frac{v\delta t}{\delta x} \leqslant 1, \tag{10}$$

where v is the speed of travel for the 1D explicit approximation in Eq (9) to ensure the numerical integration is accurate to compute the correct values of every step. For implicit time stepping or more complicated method, different CFL limits are used and larger time steps may be tolerated.

Flow tracer could be used to track the flow of the fluid. PLUTO allows adding "colors" Q_k to the fluids to distinguish initialized layers. The advection of the tracer follows

$$\frac{\partial(\rho Q_k)}{\partial t} = \nabla \cdot (\rho Q_k \boldsymbol{v}). \tag{11}$$

The initialization of PLUTO use dimensionless units, such that the quantities are scaled to reasonable numbers to avoid overflow or underflow errors. Three fundamental units are required, including the density ρ, the length L and the velocity v with c.g.s unit gr/cm^3, cm and cm/s respectively. The unit other quantities could be derived

from the above unit, for instant, time t in s and pressure P in gr/cm/s^2. The quantities are dimensionless after dividing the fundamental constant $\rho_0 = 1m_p$ =gr/cm^3, $L_0 = 1$ AU, $v_0 = 1$ km/s, which could be re-defined for specific problems.

IV. THE SOUND WAVE PROPAGATION

Sound wave is a longitudinal wave, which propagates forward by making compression and rarefraction. It could be represented by an adiabatic system which has small perturbation about the equilibrium, resulting in energy transfer. The heat exchange could be neglected as the time scale of heat conduction is much smaller than that of the wave propagation.

A. The sound wave equation

By giving a push to the system, the disturbance displaces the fluid initially in equilibrium state with equilibrium density ρ_0, equilibrium pressure P_0 and zero fluid velocity $\boldsymbol{v}$,such that:

$$P = P_0 + P', \rho = \rho_0 + \rho', \boldsymbol{v} = \boldsymbol{v}', \tag{12}$$

where ρ', P' and $\boldsymbol{v}'$ are the perturbed quantities respectively. Using the above relations, the continuity equation (2) and the momentum equation (5) could be written as

$$(\rho_0 + \rho')(\frac{\partial \boldsymbol{v}'}{\partial t} + \boldsymbol{v}' \cdot \nabla \boldsymbol{v}') = -\nabla(P_0 + P'), \tag{13}$$

$$\frac{\partial}{\partial t}(\rho_0 + \rho') = -\nabla \cdot ((\rho_0 + \rho')\boldsymbol{v}'). \tag{14}$$

Using the method of linearization while assuming the perturbation is small, such that the higher-order terms could be neglected, Eq (13) and Eq (14) could be rewritten as

$$\rho_0 \frac{\partial \boldsymbol{v}'}{\partial t} = -\nabla P', \tag{15}$$

$$\frac{\partial \rho'}{\partial t} + \rho_0 \nabla \boldsymbol{v}' = 0. \tag{16}$$

For the adiabatic wave propagation in air, we could assume the air is as ideal diatomic gas, where the adiabatic index $\gamma = 1.4$. From the relation

$$PV^\gamma = constant, \tag{17}$$

where $V = m/\rho$ is the volume of gas with mass m, take the derivative and obtain

$$\frac{dP}{d\rho} = \gamma \frac{P}{\rho} \tag{18}$$

Using Eq (15), Eq (16) and Eq (18) with some manipulation, we obtain the equation of pressure and the density:

$$\frac{\partial^2 P'}{\partial t^2} = \gamma \frac{P_0}{\rho_0} \nabla^2 P', \tag{19}$$

$$\frac{\partial^2 \rho'}{\partial t^2} = \gamma \frac{P_0}{\rho_0} \nabla^2 \rho', \tag{20}$$

which satisfy the 3D wave equation with

$$c_s^2 = \gamma \frac{P_0}{\rho_0}, \tag{21}$$

is the speed of sound.

In 1D, it could be shown that the solutions for the wave equations are

$$P' = \alpha c_s^2 \cos(kx - \omega t), \tag{22}$$

$$\rho' = \alpha \cos(kx - \omega t), \tag{23}$$

$$v' = \alpha \frac{c_0}{\rho_0} \cos(kx - \omega t), \tag{24}$$

for the wave propagating in the $+x$ direction, where k is the wavenumber and ω is the frequency.

By substituting Eq (22) into the wave equation, the dispersion relation of waves $\omega^2 = c_s^2|k|^2$ could be obtained, which defines the relation between ω and k.

The initialization of the quantities are as follows:

$$\rho = \rho_0 + \sigma \cos(kx), \tag{25}$$

$$P = P_0 + \sigma c_s^2 \cos(kx), \tag{26}$$

$$v = \sigma \frac{c_s}{\rho_0} \cos(kx), \tag{27}$$

with $\rho_0 = P_0 = 1$,$k = 2\pi$, $c_s = \sqrt{\gamma \frac{P_0}{\rho_0}}$ with $\gamma = 1.4$ and σ is the size of perturbation. Three σ values were tested, including 0.0001, 0.2 and 0.5 to analysis the non-linearity if the initial disturbance is comparable to the equilibrium state.

The x-direction boundaries are set to periodic to represent the infinite long 1D propagating sound wave.

B. Simulation results and discussion

Figures 2(a), 3(a) and 4(a) show the simulation results of density, pressure and velocity when a perturbation of order σ was add to the equilibrium state. When the perturbation is small, i.e. $\sigma = 0.0001$, the variables only slightly deviate from the equilibrium values, the method of linearization is a good approximation to predict the

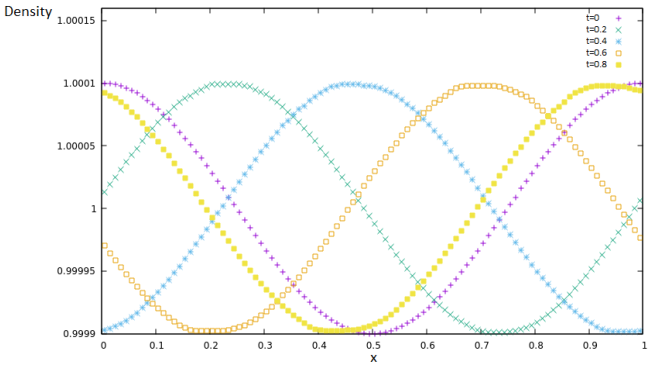

(a) $\sigma = 0.0001$

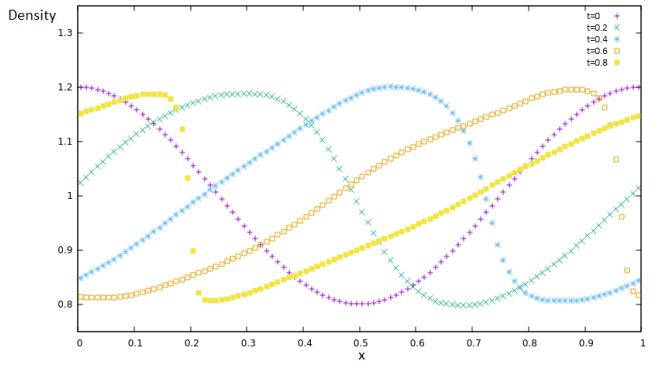

(b) $\sigma = 0.2$

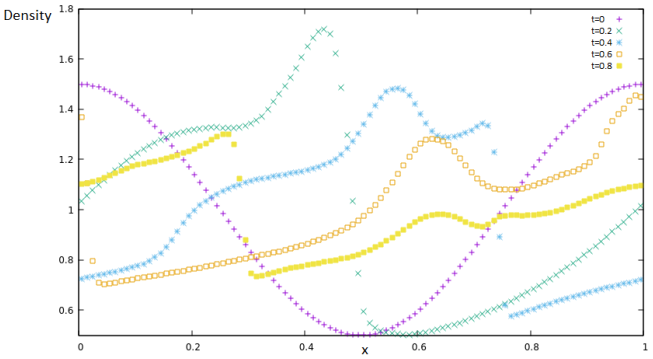

(c) $\sigma = 0.5$

FIG. 2: The density plots along the x-axis for time t with 0.2 step within a period and different σ values

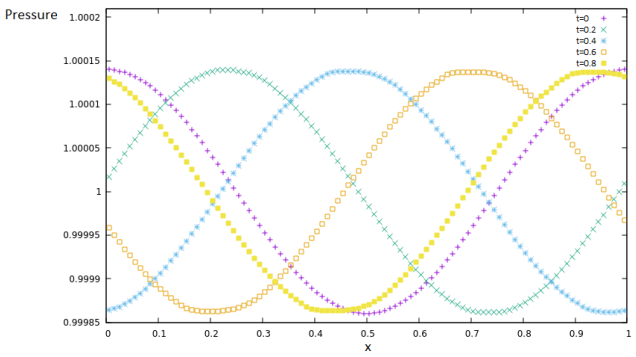

(a) $\sigma = 0.0001$

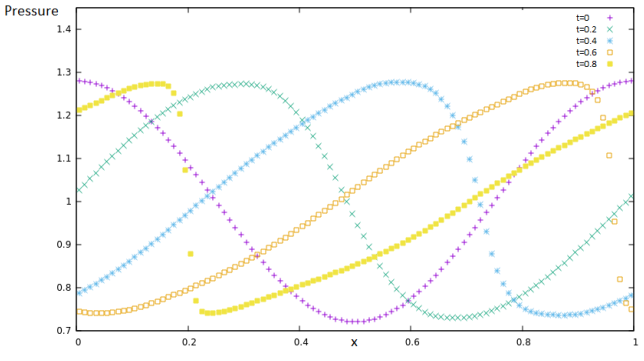

(b) $\sigma = 0.2$

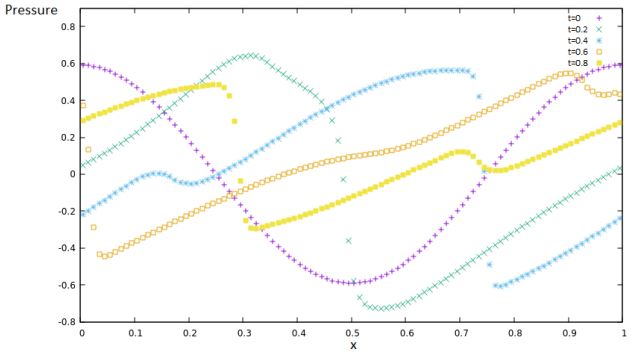

(c) $\sigma = 0.5$

FIG. 3: The pressure plots along the x-axis for time t with 0.2 step within a period and different σ value

wave propagation with the 1D wave equation. The wave propagated to the right with a constant wave speed and constant waveform with wavelength $\lambda = 1$. After $t = 1$, the wave still behave like a sinusoidal function and overlap the initial waveform once before reaching $t = 1$. Using Matlab fitting function, figure 5 shows the fitting result. Comparing the density plot at $t = 1$ with the initial condition, ω is determined as 7.43. The speed of sound therefore is $c_s = \frac{\omega}{k} = 1.18$, which agrees with $c_s = \sqrt{\gamma \frac{P_0}{\rho_0}} = 1.18$ code units with an error of 0.02%.

Figures 2(b), 3(b) and 4(b) show the plots with $\sigma = 0.2$, which the perturbation is comparable to the equilibrium state. In this case, the linearization approximation has broken down since the second-order terms become significant. The wave equation no longer holds for the sound wave propagation. Eq (21) is an approximation to the expression of the sound wave speed c_s, which ignores the negligible perturbation term when deriving the wave equation. However, when the perturbation is comparable to the equilibrium value, the sound wave speed is in fact

$$c_s = \sqrt{\gamma \frac{P}{\rho}} = \sqrt{\gamma \frac{P_0 + P'}{\rho_0 + \rho'}}. \tag{28}$$

As a result, the wave speed is not uniform over the length. Figure 2(b), 3(b) and 4(b) shows that the upper part of

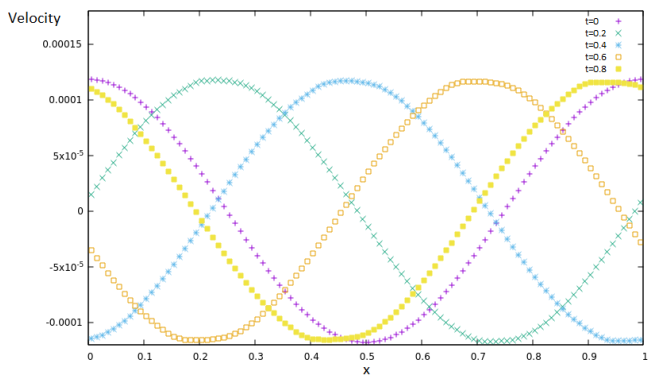

(a) $\sigma = 0.0001$

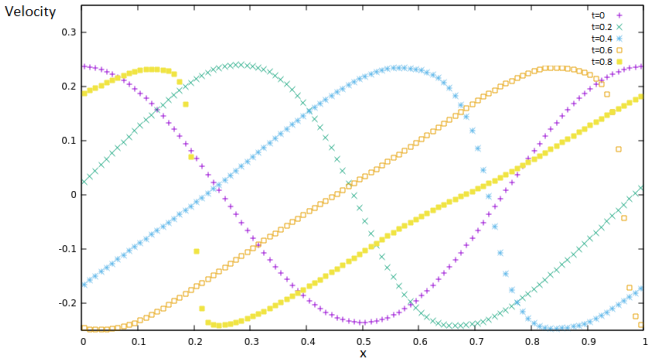

(b) $\sigma = 0.2$

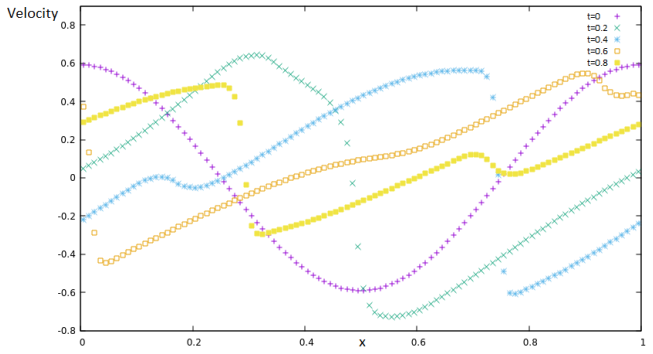

(c) $\sigma = 0.5$

FIG. 4: The velocity plots along the x-axis for time t with 0.2 step within a period and different σ values

the waves travel faster and the lower part of the waves travel slower due to different c_s for all plots.

When the perturbation terms were tuned even larger, to $\sigma = 0.5$, the nonlinear terms significantly perturb the equilibrium state, leading to the distorted waves shown in figure 2(c), 3(c) and 4(c). The sudden change in pressure, density and velocity leads to a shock and the waveform quickly show nonlinear effects. Other than the phenomenon observed for the $\sigma = 0.2$ case, the case with stronger disturbance shows change in the sinusoidal wave. The amplitudes decrease with simulation time and the plots shown composites of wave as there are more than one peak and one trough when the wave propagates.

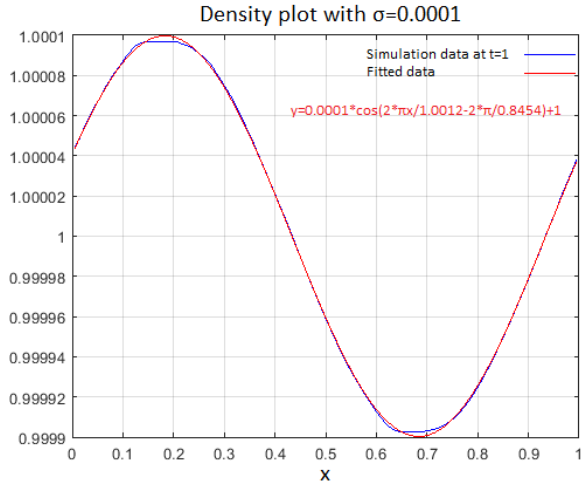

FIG. 5: The cosine fit for density plot with $\sigma = 0.0001$ at $t = 1$

Therefore, the equations (19) and (20) could only hold for the weakly perturbed systems, where the perturbation terms are not comparable to the equilibrium states. If not, correction should be made to the equations and the higher order terms should be included to predict the wave propagation characteristics.

V. THE SOD SHOCK TUBE PROBLEM

Another famous 1D problem related to computational fluid dynamics is the Sod Shock tube problem, which was named after Sod, who tested the accuracy of different computational codes by comparing to the analytical results[3]. The system of fluid at rest is divided into two parts with two different states which are separated by a membrane initially. The membrane is removed and the two parts are allowed to mix together to study the change in the conservative quantities. The discrepancies between the analytical solution and the numerical simulation arise due to the discontinuity of first derivative when shock and contact discontinuity are produced. Sod's work was reproduced to test the PLUTO code and compare with the analytical solution.

A. Characteristics and analytical solution

The three characteristics of the Sod shock tube are the rarefraction wave, contact discontinuity and the shock wave, where the rarefraction wave travels to the zone with higher pressure and density, the contact discontinuity and the shock wave travels to the opposite direction[4]. Figure 6 shows the expected phenomenon when the membrane between the left and right states is removed, assuming the left state has higher pressure and velocity. The pressure difference between the states leads

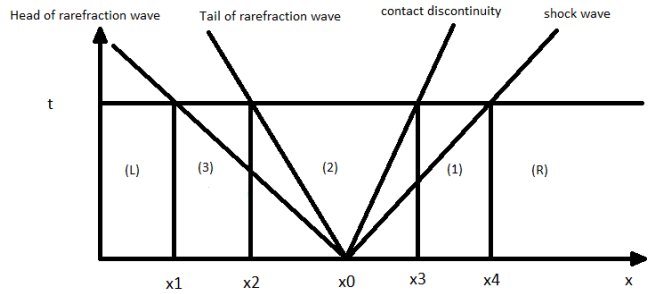

FIG. 6: The exact solution at time t for the Sod shock tube problem.

to the shock wave propagating to the right and the rarefraction wave propagating to the left from x_0 initially, with constant velocities, such that the states in area beyond $x1$ and x_4 keep unchanged. Using Eq (28), the wave speed of the head of rarefraction wave $c_1 = \sqrt{\gamma \frac{P_L}{\rho_L}}$ and the wave speed of shock wave $c_4 = \sqrt{\gamma \frac{P_R}{\rho_R}}$ could be obtained, where P_L, ρ_L, P_R and ρ_R are the pressure and density of the left and right states respectively, assuming $P_L > P_R$ and $\rho_L > \rho_R$.

The density ρ_1, pressure P_1 and the velocity v_1 are discontinuous at the shock wave front. It could be shown that:

$$\frac{P_1}{P_R} = \frac{2\gamma}{\gamma+1} M_s^2 - \frac{\gamma-1}{\gamma+1}, \tag{29}$$

$$\frac{\rho_R}{\rho_1} = \frac{2}{\gamma+1}\frac{1}{M_s^2} + \frac{\gamma-1}{\gamma+1}, \tag{30}$$

$$v_1 = \frac{2}{\gamma+1}(M_s - \frac{1}{M_s}), \tag{31}$$

where M_s relates to the shock wave speed, which could be solved numerically using the relations between different zones.

While the density ρ_2 is discontinuous at the contact discontinuity, the pressure P_2 and the velocity v_2 is continuous, where $P_2 = P_1$ and $v_2 = v_1$.

The information in zone (2) could be related to the left state, such that ρ_2 and v_2 could be obtained:

$$\frac{\rho_2}{\rho_L} = (\frac{P_2}{P_L})^{\frac{1}{\gamma}}, \tag{32}$$

$$v_2 = \frac{2}{\gamma-1}(c_1 - c_2), \tag{33}$$

where $c_2 = \sqrt{\gamma \frac{P_2}{\rho_2}}$.

In zone (3), using the initial condition, it could be shown that

$$v = \frac{2}{\gamma+1}(c_1 + \frac{x-x_0}{t}), \tag{34}$$

$$c = c_1 - (\gamma-1)\frac{U}{2}, \tag{35}$$

$$P = P_L(\frac{c}{c_1})^{\frac{2\gamma}{\gamma-1}}, \tag{36}$$

$$\rho = \rho_L(\frac{c}{c_1})^{\frac{2}{\gamma-1}}, \tag{37}$$

where v, c, P and ρ are continuous functions inside the zone depends on the position x.

As the rarefraction wave, contact discontinuity and shock wave have constant velocity, the positions x_1, x_2, x_3 and x_4 could be obtained from the initial position x_0:

$$x_1 = x_0 - c_1 t, \tag{38}$$

$$x_2 = x_0 + (v_2 - c_2)t, \tag{39}$$

$$x_3 = x_0 + v_2 t, \tag{40}$$

$$x_4 = x_0 + c_4 t. \tag{41}$$

The 1D Sod shock tube was initialized with $\gamma = 1.4$, $P_L = \rho_L = 1$, velocity $v = 0$ in all space, $P_R = 0.1$, $\rho_R = 0.125$ and t=0.2.

B. The simulation results and discussion

Figure 7 shows the comparison between the theoretical results and the simulation results. The simulation results show good agreement to the exact solution, although there are some inevitable errors due to the finite-volume methods. There are rounded-corners at the discontinuity in all graphs relate to the first-order discontinuity. The contact discontinuity of density plot overshoots and there are several points beyond the exact solutions. In general, the error of density is larger than that of pressure and velocity due to contact discontinuity.

Simulations using different grid spacing δx were performed, where the number of points along the domain N varies from 256 to 8192. The L^1 error norm (L1-norm) was calculated by

$$\frac{\sum_{i=1}^{N} |\boldsymbol{U}_{sim,i} - \boldsymbol{U}_{ana,i}|}{N}, \tag{42}$$

which is the average absolute error between the simulation results and the analytical results of the quantities, $\boldsymbol{U}_{sim}$ and $\boldsymbol{U}_{ana}$ respectively. As first-order scheme was used, the L1-norm ϵ should proportional to N^{-1}, where N is proportional to the inverse of grid size. Taking the log from both sides,

$$\ln \epsilon \propto -\ln N \tag{43}$$

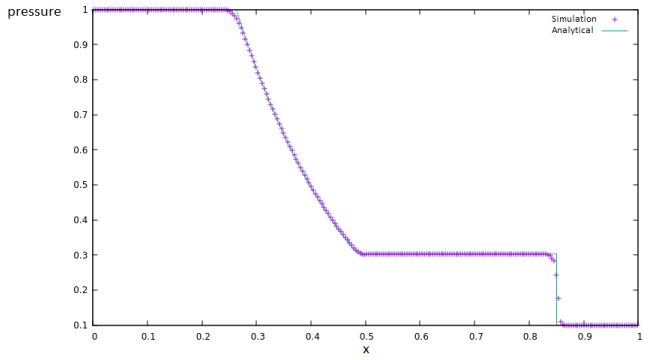

(a) Pressure

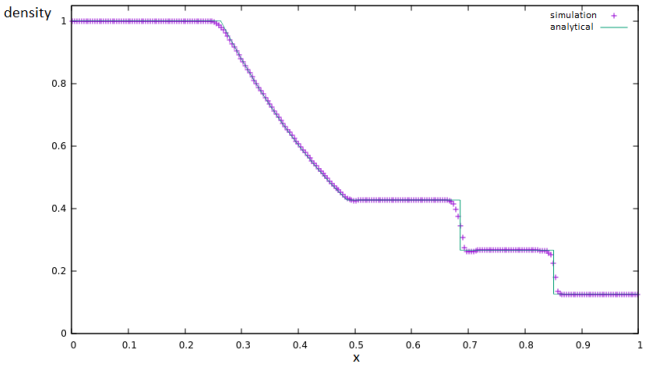

(b) Density

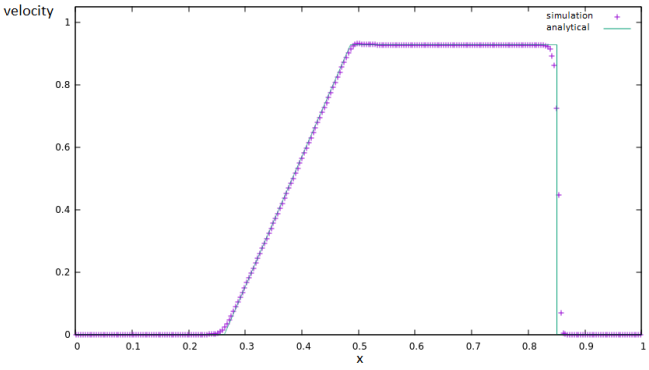

(c) Velocity

FIG. 7: The pressure, density and velocity plots for analytical and simulation results at t=0.2

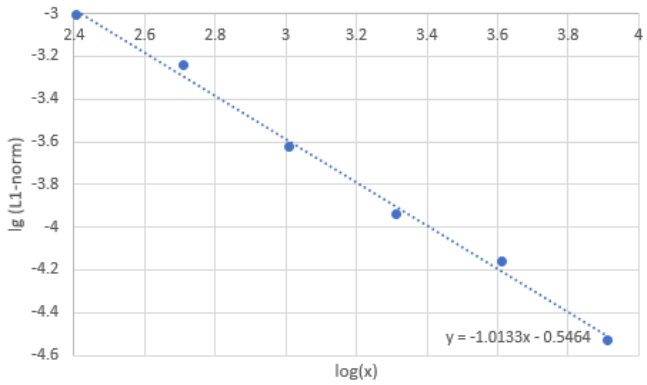

(a) Pressure

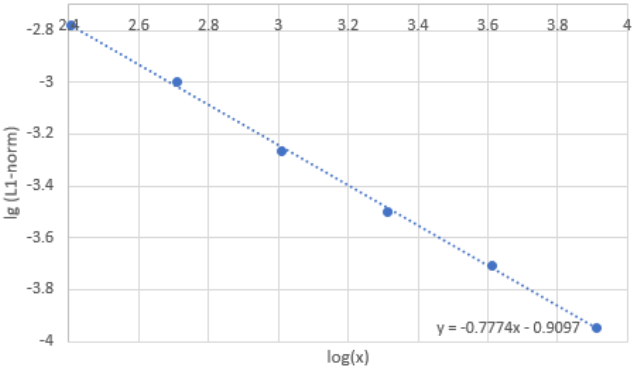

(b) Density

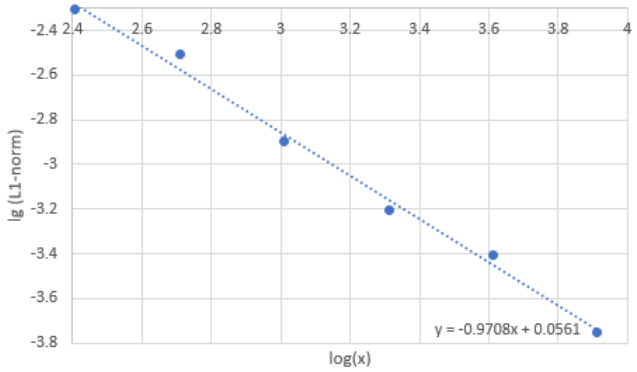

(c) Velocity

FIG. 8: The pressure, density and velocity L1 error norm plots

Figure 8 shows the plots of $\ln \epsilon$ against $\ln N$ for the variables. They show a straight line from and the slopes are -1.01 ± 0.04, -0.77 ± 0.01 and -0.96 ± 0.04 for the pressure, density and velocity respectively. As expected, the L1-norm for pressure and velocity are close to -1 while that of density was slightly greater than -1 due to the contact discontinuity.

VI. THE KELVIN-HELMHOLTZ INSTABILITY

The Kelvin-Helmholtz instability occurs along the boundary across fluid with two different properties, especially shear flow. When the shear velocity is different between the layers, small perturbation will grow over time and the interface will become unstable.

A. The dispersion relation and instabilities

Figure 9 shows the setup for Kelvin Helmholtz instability, such that fluids with different states are separated by the boundary $z = 0$. Denote the upper fluid with state 1 and the lower fluid with state 2 and consider the system

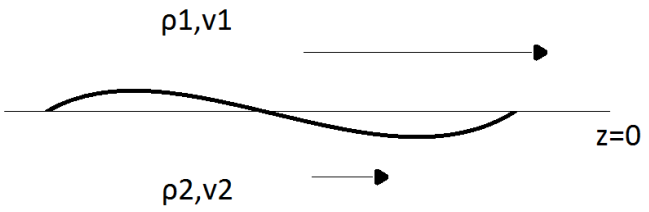

FIG. 9: The initial setup for Kelvin Helmholtz instability.

affected by the uniform gravitational field. Consider the system is perturbed in z-direction with the form:

$$z = \zeta(x) = A\exp(ikx - i\omega t), \tag{44}$$

$$\boldsymbol{u} = \boldsymbol{u}_0 + C\exp(ikx - i\omega t), \tag{45}$$

$$P = P_0 - \rho g z + P(z)\exp(ikx - i\omega t), \tag{46}$$

where $\boldsymbol{u}$ is the initial velocity, p_0 is the equilibrium pressure, $k = \frac{2\pi}{\lambda}$ is the wavenumber and ω is the angular frequency. C and $P(z)$ are the amplitudes of the perturbation. Eq (45) and Eq (46) implies the condition of perturbing the initial velocity at the boundary and the expression of pressure considering the hydrostatic component. For the incompressible and irrotational system, a scale potential ϕ could be defined where

$$\nabla^2\phi = 0, \tag{47}$$

which leads to the expression of ϕ_1 and ϕ_2 for the two states:

$$\phi_1 = C_1\exp(-i\omega t + ikx - kz), \tag{48}$$

$$\phi_2 = C_2\exp(-i\omega t + ikx + kz), \tag{49}$$

such that the perturbation tends to zero at infinity. At the interface, the pressure is continuous, such that Eq (5) becomes

$$\nabla(\frac{\partial\phi}{\partial t}) + \nabla(\frac{1}{2}\boldsymbol{u}^2) = -\frac{1}{\rho}\nabla P - \boldsymbol{g}, \tag{50}$$

which leads to the expression

$$-\rho_1(\frac{\partial\phi_1}{\partial t} + U_1\frac{\partial\phi_1}{\partial x} + g\zeta) = -\rho_2(\frac{\partial\phi_2}{\partial t} + U_2\frac{\partial\phi_2}{\partial x} + g\zeta), \tag{51}$$

At $z = 0$, Eq (51) becomes

$$\rho_1(-i\omega C_1 + ikU_1C_1 + gA) = \rho_2(-i\omega C_2 + ikU_2C_2 + gA) \tag{52}$$

Consider the deflected interface, the material derivative must be consistent such that

$$\frac{D}{Dt}\zeta = \frac{Dz}{Dt}, \tag{53}$$

implying

$$\frac{\partial\phi_1}{\partial z} = \frac{\partial\zeta}{\partial t} + U_1\frac{\partial\zeta}{\partial x}, \tag{54}$$

$$\frac{\partial\phi_2}{\partial z} = \frac{\partial\zeta}{\partial t} + U_2\frac{\partial\zeta}{\partial x}. \tag{55}$$

Substitute the expression of ζ, ϕ_1 and ϕ_2 gives

$$-kC_1 = -i\omega A + ikU_1A, \tag{56}$$

$$-kC_2 = -i\omega A + ikU_2A, \tag{57}$$

Finally, using Eq (52), Eq (56) and Eq (57), the dispersion relation could be obtained:

$$\left[\omega - k\frac{(\rho_1U_1 + \rho_2U_2)}{\rho_1 + \rho_2}\right]^2 = \frac{(\rho_2 - \rho_1)gk}{\rho_1 + \rho_2} - \frac{\rho_1\rho_2(U_1 - U_2)^2k^2}{(\rho_1 + \rho_2)^2}. \tag{58}$$

Solving Eq (58),

$$\omega = \frac{1}{2}\left[k(U_1 + U_2) \pm \sqrt{gk\frac{(\rho_2 - \rho_1)}{\rho_1 + \rho_2} - k^2(U_1 - U_2)^2}\right] \tag{59}$$

Eq (59) implies ω could be imaginary if

$$g\frac{\rho_2 - \rho_1}{\rho_1 + \rho_2} < k(U_1 - U_2)^2 \tag{60}$$

If Eq (60) is satisfied, The exponential term $\exp(-i\omega t)$ will grow with time and the system becomes unstable, which leads to the so-called Kelvin-Helmholtz instability.

B. Comparison of different results

The system was initialized with $\rho_1 = \rho_2 = 1$, $P = 1$, $U_1 = 0.5$, $U_2 = -0.5$ and $g = 0$. The gravitational effect was ignored and all combinations of k, U_1 and U_2 will lead to instability. Two values of k were test to compare the growth rate of the system, including $k = 2\pi$ and $k = 4\pi$

Figure 10 shows the tracer plots for $k = 2\pi$. As expected, the small perturbation grows over time the interface becomes vortex sheets.

Figure 11 shows the tracer plots for $k = 4\pi$. k is larger and faster growth rate is expected. Taking ln in both side of Eq (44),

$$\ln(\zeta) = -i\omega t + C, \tag{61}$$

where C is a bunch of constants. By locating the boundaries from $t = 0$ to $t = 0.39$ and take the average values of slope for the values $x = 0.15$ to $x = 0.50$ with a step of 0.00625, ω were determined as 0.085 and 0.081 for $k = 2\pi$ and $k = 4\pi$ respectively.

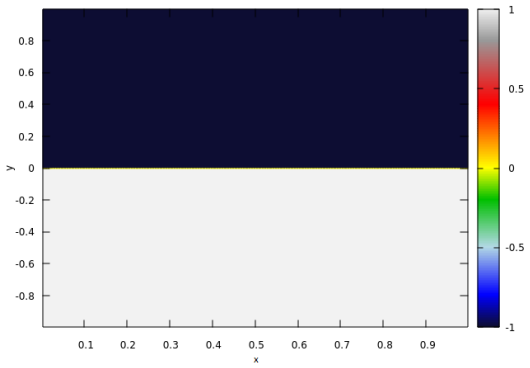

(a) $t = 0$

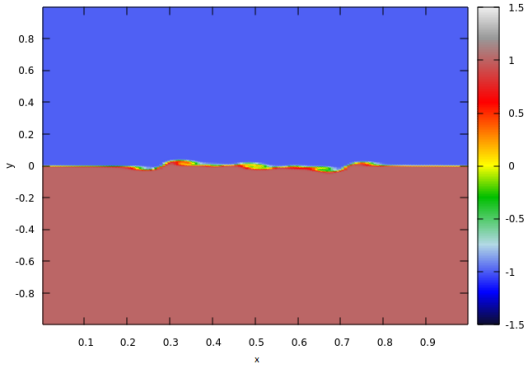

(b) $t = 0.75$

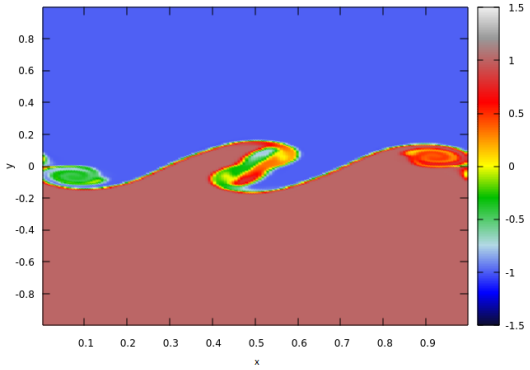

(c) $t = 1.5$

FIG. 10: The tracer plots at different time t for $k = 2\pi$

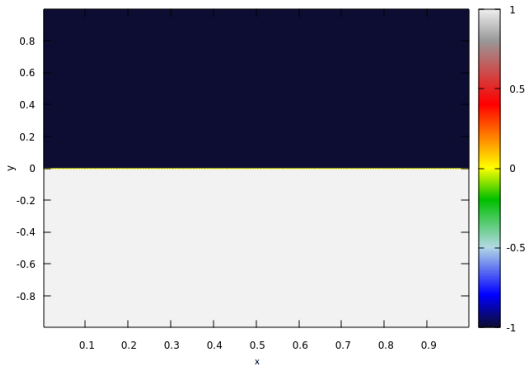

(a) t=0

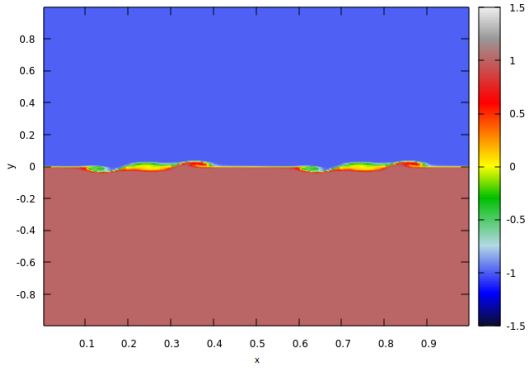

(b) t=0.75

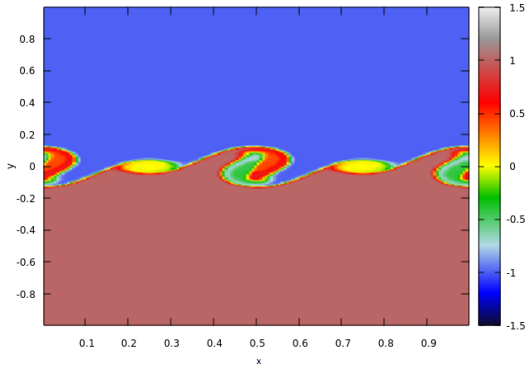

(c) t=1.5

FIG. 11: The tracer plots at different time t for $k = 4\pi$

VII. CONCLUSION AND OUTLOOK

As an introductory report to astrophysical fluid dynamics, the basic fluid dynamics equations were briefly discussed and the three problems, the sound wave propagation, the Sod shock tube and the Kelvin-Helmholtz instability were simulated and verified the theoretical results. However, hydrodynamics is only a small portion in astrophysics. Magneto or relativistic effect could be add to the hydrodynamics problem to study the non-ideal effects. In addition, the flexibility of PLUTO code allows selecting modules such as cooling, thermal conduction, viscosity, in order to investigate the real-world physics. Therefore, more complex problems could be investigated in the future with direct numerical simulation to solve theoretically mysterious physics problem.

VIII. ACKNOWLEDGEMENT

The author wishes to thank Dr. P. K. Leung from Department of Physics, The Chinese University of Hong

Kong to give advice for the project.

IX. REFERENCES

[1] Thompson, M. J., 2006. *An Introduction to Astrophysical Fluid Dynamics* (Imperial College Press:London).

[2] Mignone, A., Bodo, G., Massaglia, S., Matsakos, T.,Tesileanu, O., Zanni, C., Ferrari, A., 2007. PLUTO: A Numerical Code for Computational Astrophysics. *Astrophys. J. Suppl.*,**80**,753-790. [3]Sod, G. A. ,1978. A Survey of Several Finite Difference Methods for Systems of Nonlinear Hyperbolic Conservation Laws. *J. Comput. Phys.* **27**: 1–31. [4] C. Hirsch, 1988, *Numerical Computation of Internal and External Flows* (John Wiley Sons).